

New Measurements and Calculations on the Kinetics of an Old Reaction: $\text{OH} + \text{HO}_2 \rightarrow \text{H}_2\text{O} + \text{O}_2$

Thomas H. Speak, Mark A. Blitz,* Diogo J. Medeiros, and Paul W. Seakins*



Cite This: *JACS Au* 2023, 3, 1684–1694



Read Online

ACCESS |



Metrics & More



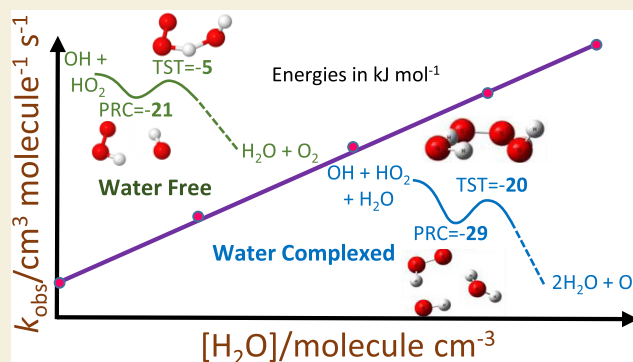
Article Recommendations



Supporting Information

ABSTRACT: Literature rate coefficients for the prototypical radical–radical reaction $\text{OH} + \text{HO}_2 \xrightarrow{k_1} \text{H}_2\text{O} + \text{O}_2$ at 298 K vary by close to an order of magnitude; such variations challenge our understanding of fundamental reaction kinetics. We have studied the title reaction at room temperature via the use of laser flash photolysis to generate OH and HO_2 radicals, monitoring OH by laser-induced fluorescence using two different approaches, looking at the direct reaction and also the perturbation of the slow $\text{OH} + \text{H}_2\text{O}_2$ reaction with radical concentration, and over a wide range of pressures. Both approaches give a consistent measurement of $k_{1,298\text{K}} \sim 1 \times 10^{-11} \text{ cm}^3 \text{ molecule}^{-1} \text{ s}^{-1}$, at the lowest limit of previous determinations. We observe, experimentally, for the first time, a significant enhancement in the rate coefficient in the presence of water, $k_{1,\text{H}_2\text{O},298\text{K}} = (2.17 \pm 0.09) \times 10^{-28} \text{ cm}^6 \text{ molecule}^{-2} \text{ s}^{-1}$, where the error is statistical at the 1σ level. This result is consistent with previous theoretical calculations, and the effect goes some way to explaining some, but not all, of the variation in previous determinations of $k_{1,298\text{K}}$. Supporting master equation calculations, using calculated potential energy surfaces at the RCCSD(T)-F12b/CBS//RCCSD/aug-cc-pVTZ and UCCSD(T)/CBS//UCCSD/aug-cc-pVTZ levels, are in agreement with our experimental observations. However, realistic variations in barrier heights and transition state frequencies give a wide range of calculated rate coefficients showing that the current precision and accuracy of calculations are insufficient to resolve the experimental discrepancies. The lower value of $k_{1,298\text{K}}$ is consistent with experimental observations of the rate coefficient of the related reaction, $\text{Cl} + \text{HO}_2 \rightarrow \text{HCl} + \text{O}_2$. The implications of these results in atmospheric models are discussed.

KEYWORDS: kinetics, radical–radical reactions, submerged barriers, tight transition states, water enhancement



INTRODUCTION

The reaction of OH with HO_2 is an important prototypical radical–radical reaction of fundamental interest and, as a chain termination process (i.e., a reaction that removes radicals), is relevant to various aspects of atmospheric¹ and combustion² chemistry, processes that are driven by free-radical chain reactions often involving OH and HO_2 .

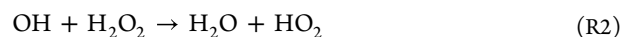


It is therefore surprising that, even though radical–radical reactions are difficult to study, literature values of the rate coefficient, k_1 , vary from approximately $(1\text{--}11) \times 10^{-11} \text{ cm}^3 \text{ molecule}^{-1} \text{ s}^{-1}$; selected examples are shown in Table 1.

High rate coefficients ($k_1 \sim (7\text{--}11) \times 10^{-11} \text{ cm}^3 \text{ molecule}^{-1} \text{ s}^{-1}$) have been obtained in several discharge flow studies with the generation of both OH and HO_2 with F-atom-based chemistry, and observation of OH by laser-induced fluorescence (LIF).^{4–7} Most recently, Assaf and Fittschen³ used an alternative technique, laser flash photolysis (LFP) of hydrogen peroxide to generate OH and excess HO_2 (HO_2 generated

indirectly via well characterized $\text{Cl}/\text{CH}_3\text{OH}/\text{O}_2$ chemistry), with OH being monitored by LIF and HO_2 by CRDS (cavity ring down spectroscopy) and determined $k_1 = (10.2 \pm 0.6) \times 10^{-11} \text{ cm}^3 \text{ molecule}^{-1} \text{ s}^{-1}$. There have also been several indirect studies involving continuous photolysis,¹⁰ molecular modulation,¹¹ and flash photolysis.¹² The 2001, IUPAC¹³ recommended value of $k_1 = (11 \pm 3) \times 10^{-11} \text{ cm}^3 \text{ molecule}^{-1} \text{ s}^{-1}$ is primarily based on the study of Keyser.⁵

Wine et al.⁸ considered reaction R1 in their study of the reaction of OH with H_2O_2



Received: March 8, 2023

Revised: May 15, 2023

Accepted: May 15, 2023

Published: June 6, 2023



Table 1. Selection of Previous Experimental Determinations of k_1

authors	$10^{11} k_1/\text{cm}^3 \text{ molecule}^{-1} \text{ s}^{-1}$	technique
Assaf and Fittschen ³	10.2 ± 0.6	laser flash photolysis (LFP), 50 Torr He. (1). Decay of OH(LIF) with excess HO ₂ (CRDS). (2). Variations in OH decays and HO ₂ yields in OH + H ₂ O ₂ reaction as initial [OH] varied. Typical $k_1' = 300 \text{ s}^{-1}$
Schwab et al. ⁴	8 ± 3	discharge flow (DF)/laser magnetic resonance (LMR) for OH and HO ₂ detection, with resonance fluorescence (RF) detection of OH, H, O. 2 Torr He. F + H ₂ O and H ₂ O ₂ , for radical generation. OH with excess HO ₂ , typical $k_1' = 20\text{--}120 \text{ s}^{-1}$
Keyser ⁵	11 ± 3	DF/RF at 1 Torr. 254–382 K. NO ₂ added to remove H and O. F + H ₂ O/H ₂ O ₂ used for radical generation. OH with excess HO ₂ , typical $k_1' = 100\text{--}300 \text{ s}^{-1}$
Sridharan et al. ⁶	7.2 ± 0.3	DF/RF at 2 Torr. 252–420 K. OH generation via H + F ₂ = HF + F, F + H ₂ O and F + H ₂ O ₂ for HO ₂ . Can measure atoms via RF and OH via LIF. OH with excess HO ₂ , typical $k_1' = 20\text{--}120 \text{ s}^{-1}$
Sridharan et al. ⁷	7.5 ± 1.2	
Wine et al. ⁸	~ 1	LFP study of OH + H ₂ O ₂ monitoring OH via LIF with excess H ₂ O ₂ , which was directly measured via UV absorption. Dramatically changed initial [OH] and saw no effect on the kinetics, consistent with $k_{1,298\text{K}} \sim 1 \times 10^{-11} \text{ cm}^3 \text{ molecule}^{-1} \text{ s}^{-1}$
Chang and Kaufman ⁹	3 ± 2	DF study of OH + O ₃ , RF lamp detection of OH and HO ₂ (via NO titration). Looking for deviation in OH traces due to secondary chemistry. OH generated by H + NO ₂

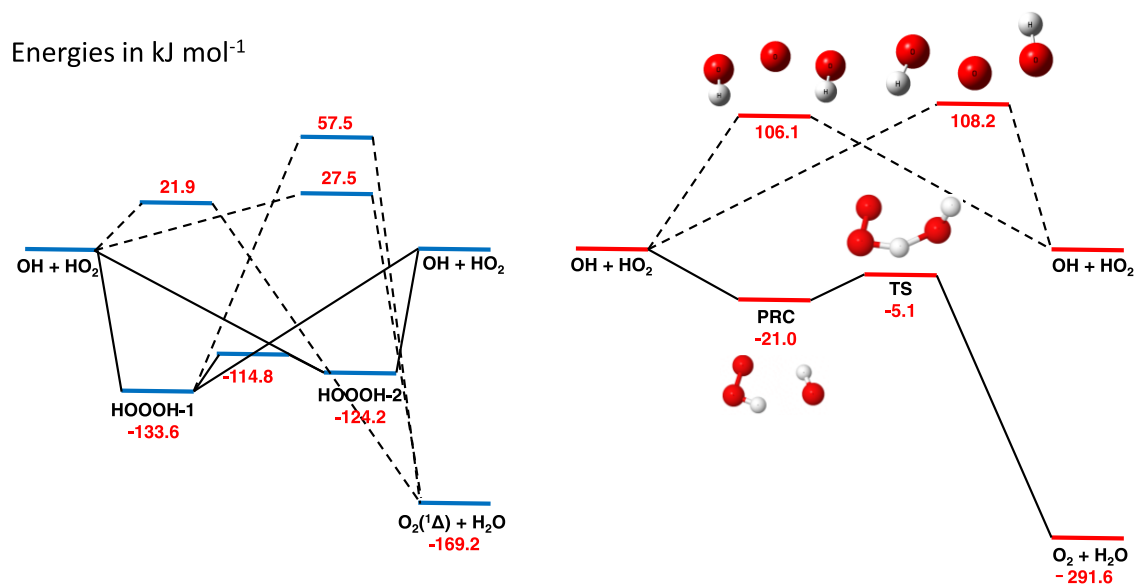


Figure 1. Singlet (left) and triplet (right) surfaces for the uncatalyzed reaction of OH and HO₂. The energies, in kJ mol^{-1} , for the singlet surface were calculated at the CCSD(T)/CBS level with the anharmonic zero point energy (ZPE) corrections calculated using the same method as used to calculate the structures (M06-2X and MP2 with the 6-311++g(3df,3pd) basis set). Triplet energy levels were calculated at the RCCSD(T)-F12b/CBS/RCCSD/aug-cc-pVTZ level.

They were aware that values of k_1 in the region of $10 \times 10^{-11} \text{ cm}^3 \text{ molecule}^{-1} \text{ s}^{-1}$ would interfere with their LFP/LIF determinations of k_2 . Wine et al. therefore added large additional concentrations of O₃ to the mix, increasing the initial concentration of both OH and HO₂ via the reactions of O(¹D), produced from O₃ photolysis, with H₂O₂



Despite increased initial radical concentrations, by a factor of up to 9, they observed no variation in the removal rate of OH, suggesting a considerably lower value for k_1 ($\leq 2.2 \times 10^{-11} \text{ cm}^3 \text{ molecule}^{-1} \text{ s}^{-1}$). A similar lack of dependence of k_2 on radical concentration was reported in a flow tube study by Keyser.¹⁴ However, Assaf and Fittschen³ also studied the reaction R2 using a similar approach to Wine et al. but with much lower [H₂O₂] and hence lower pseudo-first-order rate coefficients. In contrast, Assaf and Fittschen did observe significant perturbation of the OH decays and a reduction in the HO₂ yield consistent with a value of $k_1 \sim 10 \times 10^{-11} \text{ cm}^3 \text{ molecule}^{-1} \text{ s}^{-1}$.

Due to both significant practical and fundamental interest, there have been several theoretical studies of reaction R1.^{15–23} All studies agree that the reaction predominantly takes place on the triplet potential energy surface (PES), as shown in Figure 1, via the formation of a pre-reaction complex (PRC), stabilized ca. 13–24 kJ mol^{-1} below the entrance channel, with a submerged, but relatively tight transition state (-7 to -12 kJ mol^{-1} below the entrance channel) leading to products. Although the primary focus of several studies was kinetics at high temperatures, virtually all theoretical studies report room-temperature rate coefficients for k_1 of ca. $1\text{--}7 \times 10^{-11} \text{ cm}^3 \text{ molecule}^{-1} \text{ s}^{-1}$. Several recent studies predict that k_1 has a significant water dependence, although none has been reported from experimental measurements despite significant variations in [H₂O].^{15,18}

Although reaction via the triplet state is dominant, the excited singlet state can play a role. Badenes et al.²⁴ calculated a high barrier (56.8 kJ mol^{-1}) from the HOOH complex to the abstraction projects and hence only considered recombination. Recombination only plays a significant role at very high

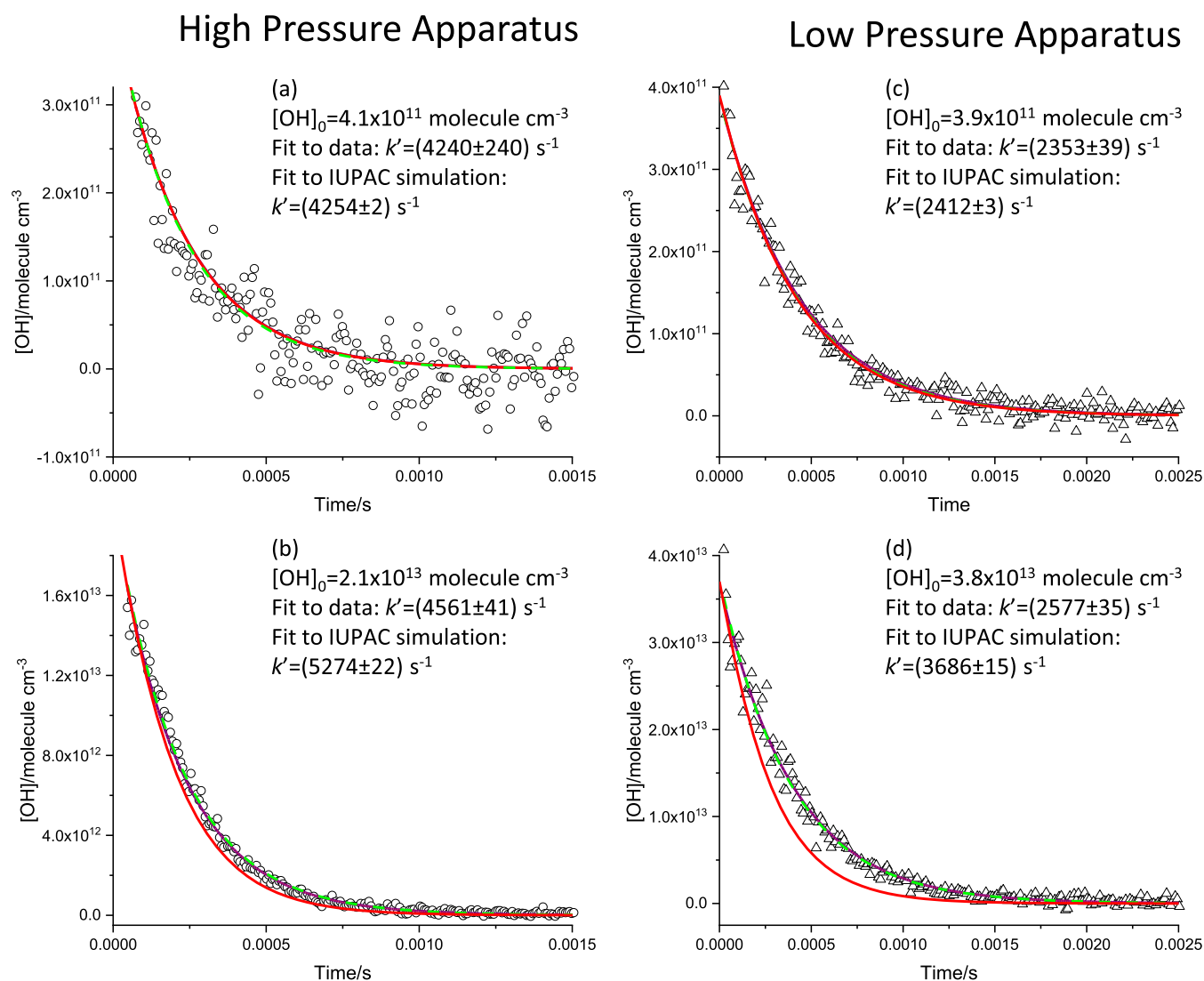


Figure 2. Four example traces with varying laser power in the two different experimental setups. Traces (a, b) from the high-pressure apparatus (1800 Torr of N_2 at 298 K, $[\text{H}_2\text{O}_2] = 2.5 \times 10^{15} \text{ molecule cm}^{-3}$). Traces (c, d) from the conventional low-pressure apparatus (200 Torr of Ar at 298 K, $[\text{H}_2\text{O}_2] = 1.4 \times 10^{15} \text{ molecule cm}^{-3}$). These traces differ in their initial OH concentration ranging from (a) $[\text{OH}]_0 = 4.1 \times 10^{11} \text{ molecule cm}^{-3}$ to (d) $[\text{OH}]_0 = 3.8 \times 10^{13} \text{ molecule cm}^{-3}$. \circ , Data points from high-pressure apparatus; Δ data points from low-pressure apparatus; (blue line), fit from global analysis; (green line), exponential fit to that single data trace; (red line) simulation using $[\text{OH}]_0$ and IUPAC rate coefficients.

pressures. More recently, Lu et al.²⁵ found a pathway on the singlet surface with a slightly submerged barrier (ca. -4 kJ mol^{-1}) and suggested that reaction on the singlet surface could contribute to $\sim 10\%$ of the reaction.

Our initial interest in reaction R1 was sparked by comments on our paper outlining the development of a new LIF instrument for OH and HO_2 detection.²⁶ We used both reaction R2 and reaction R4 to internally calibrate our OH and HO_2 LIF signals to allow us to determine HO_2 yields from OH-initiated reactions.



Both methods gave consistent results, but the slower reaction R2 calibration reaction should show a dependence on radical concentration if $k_1 \sim 10 \times 10^{-11} \text{ cm}^3 \text{ molecule}^{-1} \text{ s}^{-1}$.

In this paper, we present three laser flash photolysis/laser-induced fluorescence experiments designed to determine k_1 over a range of conditions:

- (1). Studying the variation of k_2 via LIF observation of OH using a conventional slow flow LFP/LIF system at pressures of 75–200 Torr.^{27,28}
- (2). Studying the variation of k_2 via LIF observation of both OH and HO_2 at high pressures ($\sim 1800 \text{ Torr N}_2$) as a function of initial radical concentration using our new instrumentation.²⁶
- (3). Photolyzing water in the presence of O_2 to generate equal concentrations of OH and HO_2 at high pressures ($\sim 1800 \text{ Torr N}_2$) and with varying concentrations of water to investigate the predicted water dependence of k_1 .

We support our experimental observations with calculations of the PES for R1 and analogous reactions and calculate rate coefficients using the master equation code MESMER.²⁹

METHODS

Experimental Section

All studies were carried out in two slow-flow, laser flash photolysis/laser-induced fluorescence systems (LFP/LIF), one at high pressures (typically ~1800 Torr N₂) and the other at lower pressures of 75–200 Torr (Ar or N₂). Hydrogen peroxide (50% v/v with H₂O, Sigma-Aldrich) photolysis at 248 nm was used as the photolysis source of OH radicals for most experiments. This process is well characterized and produces only ground vibrational state OH.



Calibrated energy meters were used to measure the laser fluence and hence, in combination with known precursor concentrations, estimate the initial radical concentrations. LIF was used to detect OH in both systems and details are given below. The time delay between the photolysis pulse and the LIF probe pulse was systematically varied to build up OH temporal profiles. Examples of typical OH decay traces can be seen in Figure 2. For both systems, hydrogen peroxide from a thermostatted bubbler was entrained into a flow of argon and then into the reaction chamber. Pressures in the reaction chamber were controlled by throttling the exit valve and were measured using the appropriate capacitance manometer.

High-Pressure System

Details on the high-pressure system can be found in Stone et al.³⁰ and Speak et al.²⁶ and a schematic of the apparatus is shown in Figure S1. The pre-mixed gases (H₂O₂, H₂O, and N₂) were flowed through a high-pressure tube. Photolysis (Lambda Physik Compex 200, output fluence 0.5–120 mJ cm⁻²) occurred along the axis of the high-pressure flow tube and photolysis repetition rates were varied to ensure that there were no effects on the kinetics from multiple photolyses. At the end of the tube, a portion of the gas mixture was sampled through a 1 mm diameter pinhole into a low-pressure (~3 Torr) region forming a jet. In this region, OH was monitored via LIF, exciting the radicals at 282 nm (Sirah dye laser operating on Rhodamine 6G, pumped by 532 nm output of a Quantel Q Smart 850 Nd:YAG laser) to $\nu = 1$ in the upper electronic state and monitoring the resultant fluorescence at 308 nm through a narrow band filter (308 ± 5 nm, Barr Associates) coupled with a photomultiplier tube (PMT, PerkinElmer C1943P), mounted perpendicular to the probe laser and the jet. At the point at which the jet breaks down, NO was injected to convert HO₂ into OH



with the OH produced monitored in a second LIF cell with duplicate fluorescence collecting apparatus. Flows of NO were alternated with N₂ to allow the subtraction of the residual OH reaching the second LIF cell.

Low-Pressure System

The low-pressure system was a conventional slow flow system and details can be found in Onel et al.³¹ and Glowacki et al.²⁸ and an apparatus schematic is shown in Figure S2. Argon (200 Torr) was predominantly used as the bath gas, but some experiments were carried out with nitrogen (75 Torr) as the bath gas. The photolysis laser (Lambda Physik LPX 200), probe laser (Continuum Precision II Nd:YAG pumping a Sirah dye laser operating with DCM dye), and fluorescence detection axes were mutually perpendicular. For this system, OH was probed via excitation at 308 nm to $\nu = 0$ in the first electronically excited state and the PMT (PerkinElmer C1943P) detected the resonant fluorescence.

Typically, experiments were run at 10 Hz, but checks were carried out at 2 Hz to ensure that multiple photolyses were not an issue (see Figure S4). Wire gauze filters were used to attenuate the photolysis energy from ~100 mJ pulse⁻¹ to ~1 mJ pulse⁻¹; with identical OH precursor concentrations, this resulted in a decrease of approximately a factor 100 in the initial [OH].

Supporting Calculations

Supporting rate theory and *ab initio* calculations were undertaken to complement the experimental studies. *Ab initio* calculations for the PES for reaction R1 were performed at various levels of theory using Gaussian 09³² and MOLPRO 2012³³ in order to generate energies and vibrational frequencies required for the master equation rate theory calculations. Further details on the *ab initio* calculations can be found in the SI, Section S2.

Rate coefficients are calculated using a master equation analysis of the pre-reaction complex (PRC). The capture rate coefficient for entry into the PRC is estimated using the methods of West et al.³⁴ The micro-canonical rate coefficients for re-dissociation of the complex back to reagents is determined by an inverse Laplace transform (ILT) method. The rate of the forward reaction over the well-defined transition state to products is determined by a conventional RRKM analysis. The RRKM microcanonical formulation for a unimolecular reaction is

$$k(E) = \frac{N(E)}{h\rho(E)} \quad (\text{E1})$$

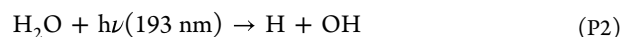
where $N(E)$ is the number of accessible states in the TS and $\rho(E)$ is the density of states of the pre-reaction complex. The calculations allow for the optical isomers of the transition state as discussed by Monge-Palacios and Sarathy.¹⁷ Calculations were implemented by the MESMER software package.²⁹ An example MESMER input file can be found in the SI, Section S9.

RESULTS

Figure 2a,b shows examples of typical OH traces following the photolysis of H₂O₂ at 248 nm to generate OH radicals and their subsequent removal by reaction R2 in the high-pressure system. The traces represent a wide range of initial [OH] (overall concentrations varied from 1.1 × 10¹¹ to 2.6 × 10¹³ molecule cm⁻³) as evidenced by the varying signal to noise. Over 54 OH and 12 HO₂ traces were taken and fitted globally to return a value of $k_1 = (1.34 \pm 0.14) \times 10^{-11}$ cm³ molecule⁻¹ s⁻¹, where the error is statistical at the 1σ level. In Figure 2, we show the results of the global analysis (purple line), along with individual exponential fits of each trace (green line, for most traces the global and local fits overlap) and the simulated profiles for $k_1 = 11 \times 10^{-11}$ cm³ molecule⁻¹ s⁻¹ (red line). In agreement with Wine et al., there is very little dependence of the pseudo-first-order rate coefficient, k_1' , with initial [OH] (varied from 4.1 × 10¹¹ to 2.1 × 10¹³ molecule cm⁻³ in the figure plots) and certainly much less than predicted based on the IUPAC recommended value (red lines).

Section S3 in the SI also contains additional example traces from similar studies on reaction R2 carried out in both apparatuses over a range of [OH]₀ and with varying laser repetition rates. Example HO₂ traces and additional information on monitoring HO₂ can be found in Figure S5 in the SI (Section S4). In the low-pressure studies, a set of wire meshes was used to vary the photolysis laser fluence from 120 to 1 mJ cm⁻² pulse⁻¹. A series of back-to-back low- and high-laser-power experiments were made; analysis of the 47 resulting traces (32 at 200 Torr of argon and 15 at 75 Torr of N₂) gave $k_1 = (1.00 \pm 0.32) \times 10^{-11}$ cm³ molecule⁻¹ s⁻¹. Examples of experimental traces with low and high initial [OH] are shown in Figure 2c,d.

For the high-pressure water photolysis experiments in the presence of oxygen, equal initial concentrations of OH and HO₂ are obtained via





Significantly higher values of k_1 were observed, but crucially, the observed rate coefficients varied with $[\text{H}_2\text{O}]$ as shown in Figure 3. Extrapolating the observed rate coefficient to zero

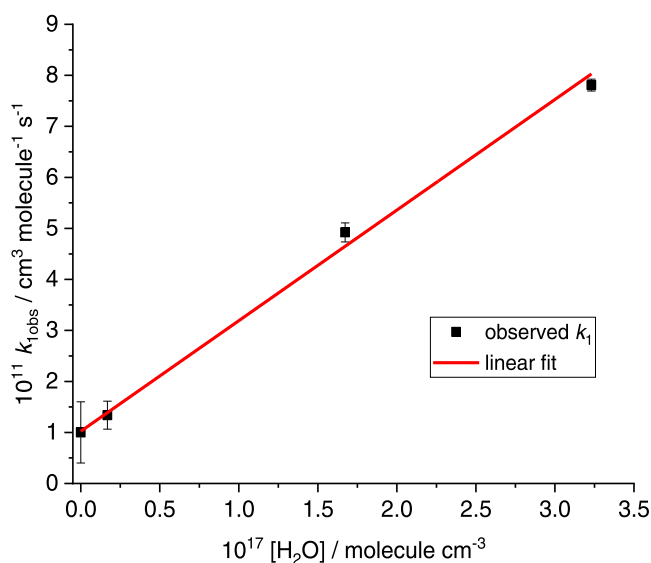


Figure 3. Plot of the observed bimolecular rate coefficient for OH and HO₂ (sum of both catalyzed and uncatalyzed) against water concentration. The black points (error bars 2σ) are the experimental values and the red line is a linear fit giving $k_{1,\text{H}_2\text{O}} = (2.17 \pm 0.09) \times 10^{-28} \text{ cm}^6 \text{ molecule}^{-2} \text{ s}^{-1}$.

water produces a value of $k_1 = (1.02 \pm 0.11) \times 10^{-11} \text{ cm}^3 \text{ molecule}^{-1} \text{ s}^{-1}$, in good agreement with our previously discussed results on the variation of the kinetics of the OH + H₂O₂ reaction as a function of initial OH concentration. Note that in the studies based on R2, some water would have been present in the system, but only at concentrations similar to that of the H₂O₂, $1\text{--}5 \times 10^{15} \text{ molecule cm}^{-3}$. Therefore, the expected enhancement based on the presence of water is only $\sim 1 \times 10^{-12} \text{ cm}^3 \text{ molecule}^{-1} \text{ s}^{-1}$, i.e., less than the uncertainty in those measurements.

The values of k_1 depend sensitively on the initial radical concentration generated. Initial radical concentrations were calculated from measured laser fluences, precursor concentrations, and literature values for the absorption cross sections and quantum yields.¹³ It is recognized that there are errors associated with these values, especially in accurately measuring low laser powers and in determining precursor concentrations. Concentrations of H₂O₂ could be constrained by the established value of k_2 ($(1.7 \pm 0.4) \times 10^{-12} \text{ cm}^3 \text{ molecule}^{-1} \text{ s}^{-1}$)¹³ at low radical concentrations, water concentrations were directly measured with a dew point hygrometer. We estimate that radical concentrations could have an uncertainty of $\sim 25\%$, but we would need to be out by a factor of $\sqrt{10}$ in the initial radical concentration of OH and HO₂ to bring our water-free results into agreement with the IUPAC recommendation.

Figure 1 shows our potential energy surface (PES) for the singlet and triplet surfaces of reaction R1. For the singlet reaction channel, calculations at the CCSD(T)/CBS//MP2/6-311++g(3df,3pd) and CCSD(T)/CBS//M06-2X/6-311++g(3df,3pd) levels were in good agreement. However, for the triplet reaction surface, it was found that the abstraction transition state structure was less certain and highly method-dependent. Table 2 shows the variation in the key parameters required for the rate coefficient calculations (a full list of frequencies can be found in the SI, Section S2 and Table S1) and the resulting room temperature rate coefficients. These different structures yielded not just differing activation barriers but also different low-frequency vibrational modes. Further work to evaluate this variability was carried out by repeating the UMP2 and M062X structures with the aug-cc-pVTZ basis sets along with calculating UCCSD/ aug-cc-pVTZ structures in Gaussian 09 and RMP2/aug-cc-pVTZ and RCCSD-F12a/aug-cc-pVTZ structures in Molpro 2012. The RMP2 and RCCSD-F12a calculations in Molpro were carried out to evaluate the influence of spin contamination as an explanation for the differing structures that had been calculated. All of these structures were then combined with extrapolated CCSD(T) single-point energies.

We have also carried out a range of calculations to investigate the observed water dependence in this study and predicted in earlier theoretical studies. As a first step, we

Table 2. Key Information for the Calculation of Rate Coefficients for the OH + HO₂ Water Free Triplet Abstraction Surface Calculated at Various Levels of Theory^a

method	A	B	C	D	E	F	G
$k_{\text{bim},300\text{K}} \text{ cm}^3 \text{ molecule}^{-1} \text{ s}^{-1}$	1.1×10^{-11}	4.7×10^{-11}	1.2×10^{-11}	9.2×10^{-11}	4.4×10^{-12}	5.8×10^{-12}	2.4×10^{-12}
TS, imaginary cm^{-1}	2658	2020	1387	1524	2441	2521	3162
TS $\nu_1 \text{ cm}^{-1b}$	251	110	205	101	397	395	292
TS $\nu_2 \text{ cm}^{-1}$	520	195	388	164	503	493	566
TS $\nu_3 \text{ cm}^{-1}$	742	458	551	475	693	694	736
TS $\nu_4 \text{ cm}^{-1}$	775	656	857	640	770	773	765
E TS kJ mol^{-1}	-5.12	-6.11	-6.71	-10.97	-2.06	-3.31	-2.98
PRC $\nu_1 \text{ cm}^{-1}$	147	148	195	206	151	149	178
PRC $\nu_2 \text{ cm}^{-1}$	204	205	217	233	225	213	227
PRC $\nu_3 \text{ cm}^{-1}$	250	257	238	252	307	286	326
PRC $\nu_4 \text{ cm}^{-1}$	422	451	413	350	503	491	499
E PRC kJ mol^{-1}	-21.00	-20.78	-21.65	-21.58	-20.51	-20.69	-19.64

^aA = RCCSD(T)-F12b/CBS//RCCSD/aug-cc-pVTZ, B = UCCSD(T)/CBS//UCCSD/aug-cc-pVTZ, C = UCCSD(T)/CBS//UM06-2X/aug-cc-pVTZ, D = UCCSD(T)/CBS//UM06-2X/6-311++g(3df,3pd), E = UCCSD(T)/CBS//UMP2/aug-cc-pVTZ, F = UCCSD(T)/CBS//UMP2/6-311++g(3df,3pd), G = RCCSD(T)-F12b/CBS//RMP2/aug-cc-pVTZ. ^bOnly the lowest frequencies are significant for rate coefficient calculations. A full listing of frequencies can be found in the SI, Table S1.

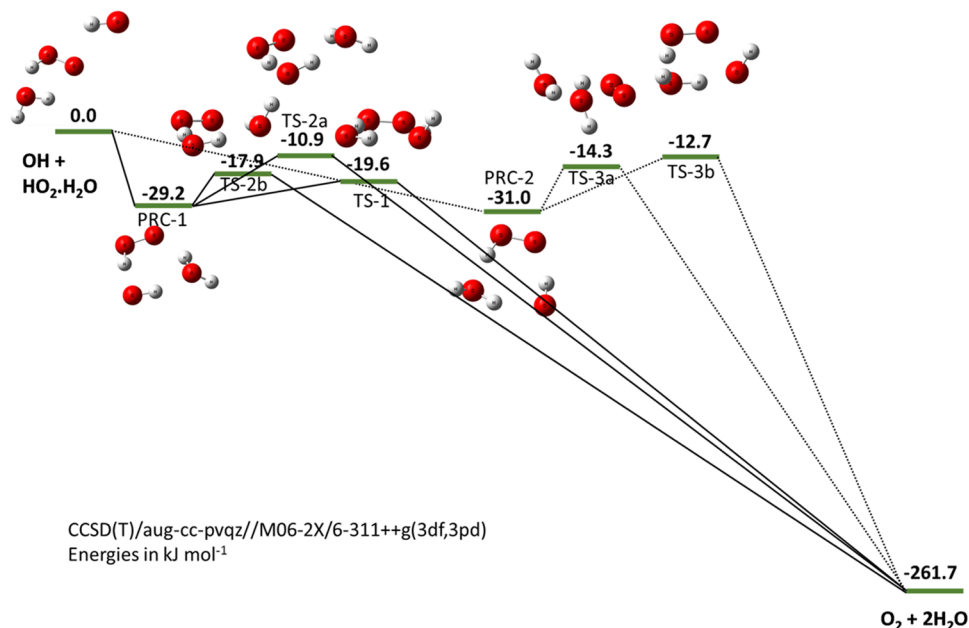


Figure 4. PES for the water-complexed system. Calculations were performed at the CCSD(T)/aug-cc-pvqz//M06-2X/6-311++g(3df,3pd) level. Note that the wells and transition states are significantly lower than for the uncomplexed system (Figure 1).

calculated the PES for $\text{H}_2\text{O}-\text{HO}_2$ complexation at the CCSD level (Section S5 and Figure S7), then, using MESMER we were able to calculate the equilibrium constant for complexation. As shown in Table S3, our calculated equilibrium constants are in good agreement with the experimental determination of Kanno et al.³⁵ From the measured water concentration, we are now able to calculate the $[\text{HO}_2-\text{H}_2\text{O}]$ and an equivalent version of Figure 3, now showing k_1' vs $[\text{HO}_2-\text{H}_2\text{O}]$ is shown in Figure S8.

The PES for the water-catalyzed surface is shown in Figure 4, where values are taken relative to the reactants OH and HO_2 complexed to water. In contrast to the uncatalyzed PES (Figure 1), there are two PRC, both of which are deeper (-29.2 or -31.0 vs -21.0 kJ mol^{-1} (Method A)). There are multiple pathways from either PRC to the products, and for each PRC, the lowest submerged barrier is significantly lower than for the un-complexed reaction (-19.6 or -14.3 vs -5.1 kJ mol^{-1} (Method A)) accounting for the significant increase in rate coefficient for the reaction of OH with water-complexed HO_2 .

DISCUSSION

Experimental Measurements

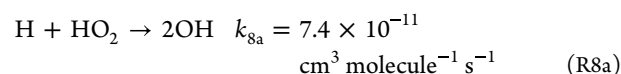
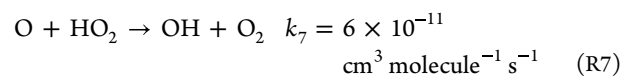
Even accounting for uncertainties associated with the initial radical concentration in these studies, there are large differences in the water-free rate coefficient for reaction R1 between this study and many other radical–radical studies. Our results are in good agreement with earlier studies on the $\text{OH} + \text{H}_2\text{O}_2$ reaction R2^{8,14} where there appears to be no interference on R2 by reaction R1, setting upper limits of $k_1 \leq 1-2 \times 10^{-11}$ $\text{cm}^3 \text{ molecule}^{-1} \text{ s}^{-1}$. Our water photolysis studies confirm the predictions of Zhang et al. that complexation of HO_2 and water significantly enhances the rate coefficient for reaction R1.

Radical–radical reactions are difficult to study, and the wide range of values for k_1 reported over the last 50 years suggest that many studies are subject to various systematic errors.

Previous studies of reaction R1 appear to have been carefully carried out, with consideration of secondary chemistry. We cannot provide an explanation for all of the variations in k_1 , and, although we have used a range of approaches in our study, we cannot rule out unknown systematic errors in our own work.

While the interference of tropospheric levels of water has a significant impact on the observed value of k_1 , water dependence cannot explain the difference with previous low-pressure flow tube measurements. According to Figure 3, $[\text{H}_2\text{O}]$ needs to be $\sim 3.5 \times 10^{17}$ molecule cm^{-3} in order to give $k_1 \sim 10 \times 10^{-11}$ $\text{cm}^3 \text{ molecule}^{-1} \text{ s}^{-1}$ which is several orders of magnitude higher than typical values in a low-pressure flow tube even when $\text{F} + \text{H}_2\text{O}$ is used to generate OH reactant radicals. However, the presence of water can partially explain the high values measured in the higher-pressure photolysis studies of Braun et al.,¹² De More¹⁰ and Cox et al.¹¹ (further discussion can be found in the SI, Section S6).

The IUPAC recommendation is primarily based on the flow tube study of Keyser.⁵ This value, $k_1 = (11 \pm 3) \times 10^{-11}$ $\text{cm}^3 \text{ molecule}^{-1} \text{ s}^{-1}$, is almost double that from a similar earlier study by Keyser³⁶ and a study by Sridharan et al.⁶ and higher than another, higher-pressure, flow tube study by Schwab et al.⁴ (Table 1). Keyser attributed the new higher value due to the presence of atomic species, O and H, which can regenerate OH via secondary chemistry¹³



However, both the flow tube systems of Schwab et al.⁴ and Sridharan et al.⁶ were specifically set up to monitor atomic species as well as OH, so it would be surprising if there were significant atomic impurities in these studies. Additionally, although both the Keyser and Sridharan et al. studies report

Table 3. PES Parameters for Reaction R1 from Various Studies

references	theory level	energy of pre-reaction complex (kJ mol ⁻¹)	energy of transition state (kJ mol ⁻¹)	10 ¹¹ k ₁ /cm ³ molecule ⁻¹ s ⁻¹
Liu et al. ²²	CCSD(T)-F12a/AVTZ	-24.5	-6.1	16.6 RPMD ^a ~3.5 QD ^b
Liu et al. ¹⁹	CCSD(T)-F12a/AVTZ	-13.6	-6.7	~3.5
Zhang et al. ¹⁸	CCSD(T) aug-cc pVTZ/	-20.9	-12.5	6.64
Monge-Palacios and Sarathy ¹⁷	CCSD(T)W3X	-13.4	-10.0	5.6
Burke et al. ¹⁶	MS-CASPT2/CBS//MS-CASPT2/ aug-cc-pVTZ			5
Zhang et al. ¹⁵	CCSD(T) aug-cc pVTZ	-24.0	-2.8	2.3
this work—method A	RCCSD(T)-F12b/CBS//RCCSD/ aug-cc-pVTZ	-21.0	-5.1	1.1
this work—method B	UCCSD(T)/CBS//UCCSD/aug-cc- pVTZ	-20.8	-6.1	4.7

^aCalculated using ring polymer molecular dynamics. ^bCalculated using quantum dynamics.

negative activation energies, the activation energy of the Keyser study is almost a factor of 2 lower, and both temperature dependencies are significantly lower than theoretical predictions. Could heterogeneous chemistry be responsible for the variation in rate coefficients between such studies and with this study? The flow tube studies do use water for radical generation and while the water concentration is insufficient to enhance the gas phase chemistry, water could promote a heterogeneous process.

Heterogeneous chemistry cannot explain the laser flash photolysis results of Assaf and Fittschen.⁵ Their study involves two approaches, a direct generation of OH and HO₂ following photolysis of H₂O₂/(COCl)₂/CH₃OH/O₂ mixtures to generate OH directly and HO₂ by the well understood Cl/CH₃OH/O₂ system giving an excess of HO₂; OH decays were followed by LIF and the concentration of HO₂ was monitored by IR cavity ring-down spectroscopy (CRDS). Second, by probing the secondary chemistry in the OH + H₂O₂ reaction which is discussed below. We have no explanation for the difference between our values and the direct study of reaction R1 by Assaf and Fittschen, in both cases HO₂ is monitored and the second-order decay of HO₂ constrains the [HO₂].

There are a range of indirect determinations of k₁ via a study of reaction R2, the reaction of OH with H₂O₂. At high conversions of OH to HO₂, reaction R1 can start to compete with reaction R2 for OH radicals, enhancing the loss of OH. As reaction R2 is relatively slow (k_{2,298K} = 1.7 × 10⁻¹² cm³ molecule⁻¹ s⁻¹)¹³ and was the subject of some uncertainty in the early 1980s, studies of reaction R2 took great care in either keeping radical concentrations very low, or checking that values of k₂ were independent of the initial radical concentration.

One of the earliest such studies was a flow tube study by Keyser.¹⁴ The value of k₂ reported in this work (k_{2,298K} = (1.64 ± 0.32) × 10⁻¹² cm³ molecule⁻¹ s⁻¹) is in excellent agreement with other studies. Typical pseudo-first-order decays were 100–200 s⁻¹ with a statistical error in the linearized slopes of 1–2% and the reaction was followed over several lifetimes, therefore for a substantial part of the OH decay, [HO₂] > [OH]. At the highest radical concentrations used (6.6 × 10¹¹ molecule cm⁻³) R1 should have contributed significantly to the OH decay (~25% enhancement) for k₁ ~ 10 × 10⁻¹¹ cm³ molecule⁻¹ s⁻¹, but no effect was observed.

Reaction R2 was also studied in flash photolysis experiments. Kurylo et al.³⁷ varied initial radical concentrations by a factor

of 5 and reported no variation in the pseudo-first-order rate coefficient. However, their initial OH radical concentration was low so that even with k₁ ~ 10 × 10⁻¹¹ cm³ molecule⁻¹ s⁻¹, the effect on k₂' would be close to the detection limit.

As discussed in the introduction, Wine et al.⁸ took a more robust approach, generating large initial concentrations of OH and HO₂ via ozone photolysis to produce O(¹D) followed by reaction R3



No variation in k₂' was observed. We have simulated the data in the Wine et al. study and this independence of the observed k₂' is again consistent with k₁ = 1 × 10⁻¹¹ cm³ molecule⁻¹ s⁻¹.

In contrast, Assaf and Fittschen³ did see a significant variation in k₂' in their study, in line with k₁ = 10 × 10⁻¹¹ cm³ molecule⁻¹ s⁻¹. Once again, careful checks have been carried out and the results seem to be consistent across a range of conditions, so there is no obvious explanation for the difference in k₁. The concentration of H₂O₂ used was significantly lower than in this and other LFP studies so that k₂' is around 300 s⁻¹, raising the possibility that other secondary reactions could contribute. The effect of reaction R1 should have an induction period while [HO₂] builds up, but this is not discernible in the traces shown.

In summary, our experimental determination of k₁ contradicts a large number of direct and indirect studies of the OH + HO₂ reaction (comparisons with other studies are covered in more detail in Section S6 in the SI). We can partially rationalize some differences due to water effects and differences between the flow tube studies suggest that systematic errors (possibly due to heterogeneous processes) may be present. Our values for k₁ are in good agreement with at least two experimental studies of the OH + H₂O₂ reaction,^{8,14} where significant variations of k₂' should have been observed if k₁ is ~10 times our observed value, but were not. Although such studies are a less direct way of determining k₁, experimentally they are much simpler to carry out, and so less subject to systematic errors. In the absence of any definitive experimental evidence, we now turn to calculations and see what light they cast on Reaction R1.

Theoretical Calculations

Table 3 summarizes previous calculations on Reaction R1. Qualitatively, all recent calculations produce a very similar PES characterized by the formation of a weakly bound pre-reaction complex (PRC) followed by the crossing of a relatively “tight”

transition state to form products. The variation in key PES parameters illustrated in Table 3 was the driving force in our systematic exploration of reaction R1 at various levels of theory. As with the experimental values, our calculations of k_1 are lower than those in the literature; however, virtually all of the literature values are at least approximately a factor 2–5 lower than the IUPAC recommended value.

Once the PRC is formed, there is a competition between re-dissociation and product formation. Although the barrier to product formation is lower, this transition state is tighter compared to re-dissociation. The RRKM microcanonical formulation for a unimolecular reaction is

$$k(E) = \frac{N(E)}{h\rho(E)} \quad (\text{E1a})$$

where the terms were defined earlier. The number of states, $N(E)$, in the loose TS for re-dissociation dominates over the number of available states in the tighter TS for product formation and therefore only a fraction of the PRC complexes formed lead to reaction.

Our calculated value of k_1 depends on a number of factors: the capture rate coefficient for PRC formation (relatively unimportant at temperatures of 300 K and above), the depth of the PRC and the TS to products, and the vibrational frequencies (especially low-frequency vibrations and hindered rotors) of the PRC and TS. In Table 2 we summarized the values of k_1 as a function of *ab initio* methodology. While there is some variation in k_1 , unrealistic parameter values are required to generate values of k_1 greater than $5 \times 10^{-11} \text{ cm}^3 \text{ molecule}^{-1} \text{ s}^{-1}$. The value of k_1 calculated *via* MESMER can be considered as a lower limit in that it assumes a fully statistical distribution of energy. Trajectory calculations, such as those run by Liu et al.,^{19,22} have no such limitations, although they do require a complete PES. Liu et al.¹⁹ unfortunately do not compare their trajectory calculations with transition state theory on the same PES. The more recent study of Liu et al.²² is based on their earlier PES, but with a deeper pre-reaction complex. The rate coefficient calculated using ring polymer molecular dynamics (RPMD) produces a value for $k_{1,300\text{K}}$ of $1.66 \times 10^{-10} \text{ cm}^3 \text{ molecule}^{-1} \text{ s}^{-1}$, in agreement with the recommended IUPAC value. However, Liu et al. note that their RPMD calculated rate coefficient is approximately a factor 3 greater than that calculated by Song et al.²³ using the same RPMD method but with a very slightly different PES. This variation highlights the sensitivity of k_1 to the subtleties of the PES.

Burke et al.¹⁶ report a value of $k_1 = \sim 5 \times 10^{-11} \text{ cm}^3 \text{ molecule}^{-1} \text{ s}^{-1}$ for reaction R1 at 300 K, based solely on their *ab initio* calculations, but fitting to other experimental parameters of the system they were investigating, raises this to $k_1 = \sim 10 \times 10^{-11} \text{ cm}^3 \text{ molecule}^{-1} \text{ s}^{-1}$. Their uncertainty analysis indicated that at 300 K, there was a factor 2–3 uncertainty in k_1 ; therefore, the increase of approximately a factor 2 to match room-temperature literature values of $k_1 = \sim 10 \times 10^{-11} \text{ cm}^3 \text{ molecule}^{-1} \text{ s}^{-1}$ is not unreasonable, but of course that same factor 2–3 uncertainty also encompasses much lower values consistent with our measurements.

Lastly, the initial calculation of Zhang et al.¹⁵ on the PES for reaction R1 reported a lower value of $k_1 = 2.2 \times 10^{-11} \text{ cm}^3 \text{ molecule}^{-1} \text{ s}^{-1}$. This earlier PES had a much higher barrier for product formation (-2.8 kJ mol^{-1}), and therefore this low value is not surprising. Interestingly their calculations predict a

very limited temperature dependence. A more recent calculation by the same group in 2018¹⁸ returns a much lower energy barrier ($-12.5 \text{ kJ mol}^{-1}$) and a higher rate coefficient at 300 K ($k_1 = 6.64 \times 10^{-11} \text{ cm}^3 \text{ molecule}^{-1} \text{ s}^{-1}$). The focus of the study of both Zhang et al.^{15,18} papers is the role of water in enhancing the rate of reaction R1. In both studies a significant increase in k_1 with water is predicted, consistent with the experimental observations of this work and experiment and theory on other HO₂ reactions, such as the self-reaction.

The sensitivity of k_1 to the PES (magnitude of well depth, barrier height, and low-frequency vibrations) means that even typical uncertainties in high-level calculations (e.g., $<4 \text{ kJ mol}^{-1}$ in barrier heights) lead to wide variations in the calculated rate coefficients, at least a factor of 3, whether rate coefficients are calculated using dynamical or statistical approaches. The variation in the calculated value of k_1 using MESMER with input parameters is explored further in the SI, Section S7. Here, we vary the energy, low-frequency vibrations, and imaginary frequency from the calculations of Burke et al. input into MESMER, resulting in variation of k_1 from 2.1 to $10.5 \times 10^{-11} \text{ cm}^3 \text{ molecule}^{-1} \text{ s}^{-1}$ (see Figure S9). A similar variation is observed if we vary the parameters generated by Method A in a similar fashion, although this variation will be centered around a lower value as our barrier is less submerged than that of Burke et al. Therefore, while we note that most unadjusted calculations give $k_{1,300\text{K}}$ less than the IUPAC recommendation, but greater than our experimental determination, calculations are unable to definitively resolve the discrepancies in experimental determinations. Calculations do predict the observed significant enhancement with water.

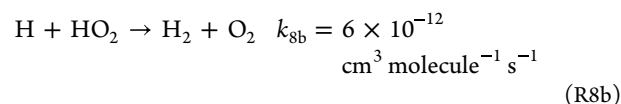
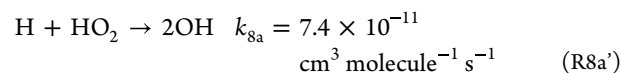
Comparison with Other Radical–Radical Reactions

Here, we compare the magnitude of k_1 with some other relevant radical–radical “abstractions” from HO₂. R7, the reaction $\text{O} + \text{HO}_2$, does have a high rate coefficient, $k_7 = 6 \times 10^{-11} \text{ cm}^3 \text{ molecule}^{-1} \text{ s}^{-1}$.



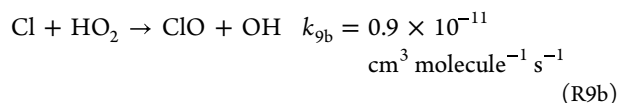
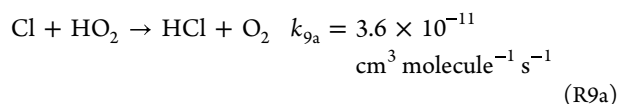
In general, OH abstractions occur with higher rate coefficients than the corresponding O reaction, tending to support a high value for k_1 ; however, isotopic studies³⁸ have shown that the mechanism of reaction R7 occurs via HOOO formation and subsequent decomposition to OH and O₂ and not by a direct abstraction; therefore, direct comparisons of k_1 and k_7 are not appropriate.

H + HO₂ also has a high rate overall coefficient ($k_8 = 8 \times 10^{-11} \text{ cm}^3 \text{ molecule}^{-1} \text{ s}^{-1}$), but once again analogies with k_1 are limited as the dominant product channel is the formation of 2OH (via decomposition of an H₂O₂ intermediate). The abstraction products H₂ and O₂, which would be formed in the analogous channel to reaction R1, are a minor channel with $k_{8b} = 6 \times 10^{-12} \text{ cm}^3 \text{ molecule}^{-1} \text{ s}^{-1}$.¹³



Reaction 9: Cl + HO₂ is the last analogy to be considered. There are two channels available with HCl + O₂ (reaction

R9a) being the dominant channel and the relevant analogy for reaction R1.³⁹



The reaction has been studied in a flow tube by Hickson and Keyser³⁹ who report a total room-temperature rate coefficient of $4.5 \times 10^{-11} \text{ cm}^3 \text{ molecule}^{-1} \text{ s}^{-1}$. In general, Cl abstraction reactions tend to be faster than the corresponding OH reaction.

We have carried out similar *ab initio* and MESMER calculations on the Cl + HO₂ reaction R9 similar to those described above for reaction R1. Qualitatively, the PES for R9 is very similar to that for R1 (see SI, Section S8 and Figure S10) with a PRC (−22.7 to −24.6 kJ mol^{−1} depending on the exact methodology) and a submerged barrier (−7.7 to −13.1 kJ mol^{−1}) to the HCl + O₂ products. Our calculations of k_{9a} , $3\text{--}4.2 \times 10^{-11} \text{ cm}^3 \text{ molecule}^{-1} \text{ s}^{-1}$, are in good agreement with experiment and larger than for the analogous OH reaction, consistent with most Cl/OH systems. The PES is also in excellent agreement with two recent calculations, both in terms of the energies of the stationary points and the kinetics for reaction R9a.^{40,41} Interestingly Zhang et al.⁴⁰ predict no significant enhancement of the rate of reaction 9 in the presence of water.

While there are fewer studies of reaction R9 than reaction R1, there are still a good number (summarized in Table S5), and in contrast to reaction R1, these all seem to be in good agreement on both the absolute rate coefficient ($k_9 = 4.2\text{--}5.3 \times 10^{-11} \text{ cm}^3 \text{ molecule}^{-1} \text{ s}^{-1}$) and the branching ratio to channel 9a (~ 0.8 , $k_{9a} = 3.2\text{--}4.5 \times 10^{-11} \text{ cm}^3 \text{ molecule}^{-1} \text{ s}^{-1}$). Studies include several flow tube measurements at low pressures and molecular modulation over the pressure range 50–760 Torr. We have no immediate explanation as to why we agree with the flow tube measurements and other studies of R9, but not for reaction R1; Cl radical generation can be carried out in the absence of water, lowering the potential for heterogeneous reactions, this hypothesis requires further evaluation. The relatively tight grouping of the experimental values for k_9 across a range of studies, suggests an absence of significant systematic errors, which may reflect the easier generation of radical reagents and the lack of enhancement by water.

Implications

Given the importance of the reaction in atmospheric chemistry, it is logical to question why such a difference in the rate coefficient has not led to significant discrepancies in measurement/model comparisons. We suspect that this is primarily due to the water dependence that has been experimentally observed for the first time in this study. Using the observed water dependence from Figure 3: $k_{1,\text{obs}} = 1.02 \times 10^{-11} + (2.17 \times 10^{-28} \times [\text{H}_2\text{O}]) \text{ cm}^3 \text{ molecule}^{-1} \text{ s}^{-1}$ gives $k_{1,\text{obs}} = 6.5 \times 10^{-11} \text{ cm}^3 \text{ molecule}^{-1} \text{ s}^{-1}$ for 1% water vapor at atmospheric pressure. This value is similar to the IUPAC recommendation at 300 K.

An important environment to consider the impact of reaction R1 is the upper atmosphere (mesosphere and

stratosphere) with typical temperatures in the range of 200–250 K. Water concentrations are low and hence water complexation cannot accelerate k_1 . However, most theoretical calculations predict much steeper increases in k_1 with decreasing temperature than are recommended by IUPAC and JPL. Therefore, the significant difference between this work and recommendations at room temperature may be reduced at temperatures relevant to the upper atmosphere. In 2017, Li et al.¹ tried to resolve the underestimation by atmospheric models ($\sim 50\%$ at 72 km) of observed HO and HO₂. An overall reduction in k_1 cannot be the simple solution to this problem, as there is better agreement lower in the stratosphere. However, the suggested solution included increasing the rate coefficient of H + O₂ + M, by up to 310%, significantly beyond the experimental uncertainties of a much simpler system than reaction R1. Further studies are required to assess the temperature dependence of both k_1 and $k_{1,\text{H}_2\text{O}}$ to assess the impact on stratospheric chemistry.

CONCLUSIONS

The rate coefficient for the reaction of OH with HO₂ has been determined via two different approaches and over a range of pressures at room temperature. The reported values ($k_1 = (1.34 \pm 0.14) \times 10^{-11} \text{ cm}^3 \text{ molecule}^{-1} \text{ s}^{-1}$ from the high-pressure studies, $(1.00 \pm 0.32) \times 10^{-11} \text{ cm}^3 \text{ molecule}^{-1} \text{ s}^{-1}$ from the low-pressure studies) are significantly lower than the IUPAC¹³ and JPL recommendations based primarily on the low-pressure flow tube work of Keyser⁵ and on more recent laser flash photolysis studies of Assaf and Fittschen.³ Theoretical studies based on a potential energy surface calculated at the RCCSD(T)-F12b/CBS//RCCSD/aug-cc-pVTZ and UCCSD(T)/CBS//UCCSD/aug-cc-pVTZ levels, combined with master equation calculations support a lower value for k_1 . However realistic variations in barrier heights and transition state frequencies, give a wide range of calculated rate coefficients.

An enhancement of the rate coefficient due to the complexation of HO₂ with H₂O has been predicted by Zhang et al.^{15,18} and is observed for the first time in this work. Such an enhancement can account for some of the experimental discrepancies, but not all. Reaction R1 is of importance in the atmosphere and the water-enhanced rate coefficients measured in this study are similar in magnitude to the IUPAC and JPL recommendations under typical tropospheric conditions, which may explain why field observations have not flagged issues around the magnitude of k_1 .

Radical–radical reactions are challenging; while we can speculate on possible reasons for some of the discrepancies in the kinetics, with the exception of studies carried out at high water concentrations, we have no concrete explanation of the differences between this and other studies. We have been careful to explore potential systematic errors, but earlier studies appear to be equally careful. Clearly, further experimental studies, particularly including temperature variation, are warranted.

ASSOCIATED CONTENT

Supporting Information

The Supporting Information is available free of charge at <https://pubs.acs.org/doi/10.1021/jacsau.3c00110>.

Experimental details including schematic diagrams; further details on the *ab initio* calculations; summary

of the experimental data; HO₂ yield data; details on the potential-energy surface and equilibrium constant of the HO₂-H₂O complex; further discussion on previous literature on reaction R1; further discussion on the sensitivity of calculated rate coefficients to input parameters; details on the Cl + HO₂ reaction (R9); and an example MESMER input file (PDF)

AUTHOR INFORMATION

Corresponding Authors

Mark A. Blitz – School of Chemistry, University of Leeds, Leeds LS2 9JT, U.K.; National Centre for Atmospheric Science, University of Leeds, Leeds LS2 9JT, U.K.; orcid.org/0000-0001-6710-4021; Email: m.blitz@leeds.ac.uk

Paul W. Seakins – School of Chemistry, University of Leeds, Leeds LS2 9JT, U.K.; orcid.org/0000-0002-4335-8593; Email: p.w.seakins@leeds.ac.uk

Authors

Thomas H. Speak – School of Chemistry, University of Leeds, Leeds LS2 9JT, U.K.

Diogo J. Medeiros – School of Chemistry, University of Leeds, Leeds LS2 9JT, U.K.; orcid.org/0000-0002-2565-4698

Complete contact information is available at: <https://pubs.acs.org/10.1021/jacsau.3c00110>

Author Contributions

CRedit: **Thomas Henry Speak** investigation, methodology, writing-review & editing; **Diogo J. Medeiros** software, writing-review & editing.

Notes

The authors declare no competing financial interest.

ACKNOWLEDGMENTS

T.H.S. was funded by the NERC Spheres doctoral training programme (NE/L002574/1). The authors are grateful to Claire Augier for help with some of the experiments. They are also grateful to Prof Michael Burke for providing details of energies and frequencies from calculations on the PES of reaction R1.

REFERENCES

- (1) Li, K. F.; Zhang, Q.; Wang, S. H.; Sander, S. P.; Yung, Y. L. Resolving the Model-Observation Discrepancy in the Mesospheric and Stratospheric HO_x Chemistry. *Earth Space Sci.* **2017**, *4*, 607–624.
- (2) Konnov, A. A. Yet another kinetic mechanism for hydrogen combustion. *Combust. Flame* **2019**, *203*, 14–22.
- (3) Assaf, E.; Fittschen, C. Cross Section of OH Radical Overtone Transition near 7028 cm⁻¹ and Measurement of the Rate Constant of the Reaction of OH with HO₂ Radicals. *J. Phys. Chem. A* **2016**, *120*, 7051–7059.
- (4) Schwab, J. J.; Brune, W. H.; Anderson, J. G. Kinetics and mechanism of the OH + HO₂ reaction. *J. Phys. Chem. A* **1989**, *93*, 1030–1035.
- (5) Keyser, L. F. Kinetics of the reaction OH + HO₂ = H₂O + O₂ from 254 to 382 K. *J. Phys. Chem. A* **1988**, *92*, 1193–1200.
- (6) Sridharan, U. C.; Qiu, L.; Kaufman, F. Rate constant of the hydroxyl+perhydroxyl (HO₂) reaction from 252 to 420 K. *J. Phys. Chem. A* **1984**, *88*, 1281–1282.
- (7) Sridharan, U. C.; Qiu, L. X.; Kaufman, F. Kinetics of the reaction OH + HO₂ = H₂O + O₂. *J. Phys. Chem. A* **1981**, *85*, 3361–3363.

(8) Wine, P. H.; Semmes, D. H.; Ravishankara, A. R. A laser flash photolysis kinetics study of the reaction OH+H₂O₂→HO₂+H₂O. *J. Chem. Phys.* **1981**, *75*, 4390–4395.

(9) Chang, J. S.; Kaufman, F. Upper bound and probable value of the rate constant of the reaction hydroxyl + hydroperoxy = water + oxygen. *J. Phys. Chem. A* **1978**, *82*, 1683–1687.

(10) DeMore, W. B. Rate constant and possible pressure dependence of the reaction OH + HO₂. *J. Phys. Chem. A* **1982**, *86*, 121–126.

(11) Cox, R. A.; Burrows, J. P.; Wallington, T. J. Rate coefficient for the reaction OH + HO₂ = H₂O + O₂ at 1 atmosphere pressure and 308 K. *Chem. Phys. Lett.* **1981**, *84*, 217–221.

(12) Braun, M.; Hofzumahaus, A.; Stuhl, F. VUV Flash Photolysis Study of the Reaction of HO with HO₂ at 1 atm and 298 K. *Ber. Bunsengesellschaft Phys. Chem.* **1982**, *86*, 597–602.

(13) Atkinson, R.; Baulch, D. L.; Cox, R. A.; Crowley, J. N.; Hampson, R. F.; Hynes, R. G.; Jenkin, M. E.; Rossi, M. J.; Troe, J. Evaluated kinetic and photochemical data for atmospheric chemistry: Volume I - gas phase reactions of Ox, HOx, NOx and SOx species. *Atmos. Chem. Phys.* **2004**, *4*, 1461–1738.

(14) Keyser, L. Absolute rate constant of the reaction OH+ H₂O₂ = HO₂+ H₂O from 245 to 423 K. *J. Phys. Chem. A* **1980**, *84*, 1659–1663.

(15) Zhang, T.; Wang, W.; Li, C.; Du, Y.; Lü, J. Catalytic effect of a single water molecule on the atmospheric reaction of HO₂ + OH: fact or fiction? A mechanistic and kinetic study. *RSC Adv.* **2013**, *3*, 7381–7391.

(16) Burke, M. P.; Klippenstein, S. J.; Harding, L. B. A quantitative explanation for the apparent anomalous temperature dependence of OH+HO₂ = H₂O+O₂ through multi-scale modeling. *Proc. Combust. Inst.* **2013**, *34*, 547–555.

(17) Monge-Palacios, M.; Sarathy, S. M. Ab initio and transition state theory study of the OH + HO₂ → H₂O + O₂ (³Σ_g⁻)/O₂ (¹Δ_g) reactions: yield and role of O₂ (¹Δ_g) in H₂O₂ decomposition and in combustion of H₂. *Phys. Chem. Chem. Phys.* **2018**, *20*, 4478–4489.

(18) Zhang, T.; Lan, X.; Qiao, Z.; Wang, R.; Yu, X.; Xu, Q.; Wang, Z.; Jin, L.; Wang, Z. Role of the (H₂O)_n (n = 1–3) cluster in the HO₂ + OH → ³O₂ + H₂O reaction: mechanistic and kinetic studies. *Phys. Chem. Chem. Phys.* **2018**, *20*, 8152–8165.

(19) Liu, Y.; Bai, M.; Song, H.; Xie, D.; Li, J. Anomalous kinetics of the reaction between OH and HO₂ on an accurate triplet state potential energy surface. *Phys. Chem. Chem. Phys.* **2019**, *21*, 12667–12675.

(20) Mozurkewich, M. Reactions of HO₂ with free-radicals. *J. Phys. Chem. A* **1986**, *90*, 2216–2221.

(21) Toohey, D. W.; Anderson, J. G. Theoretical investigations of reactions of some radicals with HO₂. 1. Hydrogen abstractions by direct mechanisms. *J. Phys. Chem. A* **1989**, *93*, 1049–1058.

(22) Liu, Y.; Song, H. W.; Li, J. Kinetic study of the OH + HO₂ → H₂O + O₂ reaction using ring polymer molecular dynamics and quantum dynamics. *Phys. Chem. Chem. Phys.* **2020**, *22*, 23657–23664.

(23) Song, Q.; Zhang, Q.; Meng, Q. Revisiting the Gaussian process regression for fitting high-dimensional potential energy surface and its application to the OH + HO₂ → O₂ + H₂O reaction. *J. Chem. Phys.* **2020**, *152*, No. 134309.

(24) Badenes, M. P.; Tucceri, M. E.; Cobos, C. J. Role of the Recombination Channel in the Reaction between the HO and HO₂ Radicals. *J. Phys. Chem. A* **2017**, *121*, 440–447.

(25) Lu, X. X.; Fu, B. N.; Zhang, D. H. Dynamics and kinetics of the OH + HO₂ → H₂O + O₂ (¹Δ_g) reaction on a global full-dimensional singlet-state potential energy surface. *Phys. Chem. Chem. Phys.* **2020**, *22*, 26330–26339.

(26) Speak, T. H.; Blitz, M. A.; Stone, D.; Seakins, P. W. A new instrument for time-resolved measurement of HO₂ radicals. *Atmos. Meas. Tech.* **2020**, *13*, 839–852.

(27) Baeza-Romero, M. T.; Glowacki, D. R.; Blitz, M. A.; Heard, D. E.; Pilling, M. J.; Rickard, A. R.; Seakins, P. W. A combined experimental and theoretical study of the reaction between

methylglyoxal and OH/OD radical: OH regeneration. *Phys. Chem. Chem. Phys.* **2007**, *9*, 4114–4128.

(28) Glowacki, D. R.; Lockhart, J.; Blitz, M. A.; Klippenstein, S. J.; Pilling, M. J.; Robertson, S. H.; Seakins, P. W. Interception of Excited Vibrational Quantum States by O₂ in Atmospheric Association Reactions. *Science* **2012**, *337*, 1066–1069.

(29) Glowacki, D. R.; Liang, C. H.; Morley, C.; Pilling, M. J.; Robertson, S. H. MESMER: An open-source master equation solver for multi-energy well reactions. *J. Phys. Chem. A* **2012**, *116*, 9545–9560.

(30) Stone, D.; Blitz, M.; Ingham, T.; Onel, L.; Medeiros, D. J.; Seakins, P. W. An instrument to measure fast gas phase radical kinetics at high temperatures and pressures. *Rev. Sci. Instrum.* **2016**, *87*, No. 054102.

(31) Onel, L.; Blitz, M. A.; Seakins, P. W. Direct Determination of the Rate Coefficient for the Reaction of OH Radicals with Monoethanol Amine (MEA) from 296 to 510 K. *J. Phys. Chem. Lett.* **2012**, *3*, 853–856.

(32) Frisch, M. J.; Trucks, G. W.; Schlegel, H. B.; Scuseria, G. E.; Robb, M. A.; Cheeseman, J. R.; Scalmani, G.; Barone, V.; Petersson, G. A.; Nakatsuji, H.; Li, X.; Caricato, M.; Marenich, A.; Bloino, J.; Janesko, B. G.; Gomperts, R.; Mennucci, B.; Hratchian, H. P.; Ortiz, J. V.; Izmaylov, A. F.; Sonnenberg, J. L.; Williams-Young, D.; Ding, F.; Lipparini, F.; Egidi, F.; Goings, G.; Peng, B.; Petrone, A.; Henderson, T.; Ranasinghe, D.; Zakrzewski, V. G.; Gao, J.; Rega, N.; Zheng, G.; Liang, W.; Hada, M.; Ehara, M.; Toyota, K.; Fukuda, R.; Hasegawa, J.; Ishida, M.; Nakajima, T.; Honda, Y.; Kitao, O.; Nakai, H.; Vreven, T.; Throssell, K.; Montgomery, J. A. J.; Peralta, J. E.; Ogliaro, F.; Bearpark, M.; Heyd, J. J.; Brothers, E.; Kudin, K. N.; Staroverov, V. N.; Keith, T.; Kobayashi, R.; Normand, J.; Raghavachari, K.; Rendell, A.; Burant, J. C.; Iyengar, S. S.; Tomasi, J.; Cossi, M.; Millam, J. M.; Klene, M.; Adamo, C.; Cammi, R.; Ochterski, J. W.; Martin, R. L.; Morokuma, K.; Farkas, O.; Foresman, J. B.; Fox, D. B. *Gaussian 09*, Revision A.0; Gaussian: Wallingford CT, 2009.

(33) Werner, H. J.; Knowles, P. J.; Knizia, G.; Manby, F. R.; Schutz, M. Molpro: a general-purpose quantum chemistry program package. *Wiley Interdiscip. Rev.: Comput. Mol. Sci.* **2012**, *2*, 242–253.

(34) West, N. A.; Millar, T. J.; Van de Sande, M.; Rutter, E.; Blitz, M. A.; Decin, L.; Heard, D. E. Measurements of Low Temperature Rate Coefficients for the Reaction of CH with CH₂O and Application to Dark Cloud and AGB Stellar Wind Models. *Astrophys. J.* **2019**, *885*, No. 134.

(35) Kanno, N.; Tonokura, K.; Koshi, M. Equilibrium constant of the HO₂-H₂O complex formation and kinetics of HO₂+HO₂-H₂O: Implications for tropospheric chemistry. *J. Geophys. Res.* **2006**, *111*, No. D20312.

(36) Keyser, L. F. Absolute rate constant of the reaction OH + HO₂ = H₂O + O₂. *J. Phys. Chem. A* **1981**, *85*, 3667–3673.

(37) Kurylo, M. J.; Murphy, J. L.; Haller, G. S.; Cornett, K. D. A flash photolysis resonance fluorescence investigation of the reaction OH + H₂O₂ → HO₂ + H₂O. *Int. J. Chem. Kinet.* **1982**, *14*, 1149–1161.

(38) Sridharan, U. C.; Klein, F. S.; Kaufman, F. Detailed course of the O + HO₂ reaction. *J. Chem. Phys.* **1985**, *82*, 592–593.

(39) Hickson, K. M.; Keyser, L. F. A kinetic and product study of the Cl+HO₂ reaction. *J. Phys. Chem. A* **2005**, *109*, 6887–6900.

(40) Zhang, T. L.; Zhang, Y. Q.; Wen, M. J.; Tang, Z.; Long, B.; Yu, X. H.; Zhao, C. B.; Wang, W. L. Effects of water, ammonia and formic acid on HO₂ + Cl reactions under atmospheric conditions: competition between a stepwise route and one elementary step. *RSC Adv.* **2019**, *9*, 21544–21556.

(41) Saheb, V.; Darijani, R. Quantum chemical and theoretical kinetics studies on the reaction of hydroperoxyl radical with chlorine atom. *Theor. Chem. Acc.* **2019**, *138*, No. 6.

Recommended by ACS

Dinitrogen Activation by Heteronuclear Bimetallic Cluster Anion FeV⁻ in the Gas Phase

Shihu Du, Ling Jiang, *et al.*

MAY 15, 2023
JACS AU

READ 

Water Charge Transfer Accelerates Criegee Intermediate Reaction with H₂O⁻ Radical Anion at the Aqueous Interface

Qiujiang Liang, Jun Yang, *et al.*

APRIL 03, 2023
JOURNAL OF THE AMERICAN CHEMICAL SOCIETY

READ 

An Experimental and Master Equation Investigation of Kinetics of the CH₂OO + RCN Reactions (R = H, CH₃, C₂H₅) and Their Atmospheric Relevance

Lauri Franzon, Arkke Eskola, *et al.*

JANUARY 05, 2023
THE JOURNAL OF PHYSICAL CHEMISTRY A

READ 

Quantitative Kinetics of HO₂ Reactions with Aldehydes in the Atmosphere: High-Order Dynamic Correlation, Anharmonicity, and Falloff Effects Are All Important

Bo Long, Donald G. Truhlar, *et al.*

OCTOBER 20, 2022
JOURNAL OF THE AMERICAN CHEMICAL SOCIETY

READ 

Get More Suggestions >